DOI: 10.1002/ejic.201100245

A Highly Zinc(II)-Selective Fluorescent Sensor Based on 8-Aminoquinoline and Its Application in Biological Imaging

Guoqiang Xie,[a] Pinxian Xi,[a] Xiao Wang,[b] Xuefei Zhao,[c] Liang Huang,[a] Fengjuan Chen,[a] Yongjie Wu,[b] Xiaojun Yao,[c] and Zhengzhi Zeng*[a]

Keywords: Sensors / Floresecent probes / Zinc / Aminoquinolines

A fluorescent probe based on 8-aminoquinoline bearing an aminophenol unit (**L1**) was developed as a chemosensor for Zn^{2+}. Sensor **L1** exhibits a high selectivity and sensitivity towards Zn^{2+} over other common metal ions in the physiological pH window and binds to Zn^{2+} through 1:1 binding mode. Fluorescent imaging of Zn^{2+} in living cells is also successfully demonstrated.

Introduction

The development of fluorescent chemosensors has attracted increasing attention because of their simplicity, sensitivity, specificity and instantaneous response.[1] It is highly demanding to selectively sense transition-metal ions, such as the zinc cation.[2] It is well known that zinc is the second-most abundant transition metal in the human body after iron and plays an important role in various pathological processes, such as Alzheimer's disease, epilepsy, ischemic stroke and infantile diarrhoea, amongst others.[3] On the other hand, Zn^{2+} does not give any spectroscopic or magnetic signals because of its $3d^{10}4s^0$ electronic configuration. It is believed that the use of fluorescence is the most effective way to detect zinc in biological systems so far.

In the last decades, considerable efforts have been made towards the design and synthesis of fluorescent chemosensors for Zn^{2+}.[4–6] Among various fluorescent sensors, 8-aminoquinoline and its derivatives were the first class of probes to be developed for Zn^{2+}.[7] They exhibit good photostability, high affinity to metal ions, and satisfactory membrane permeability.[8] Despite the availability of some commercial fluorescent probes for Zn^{2+},[9] the design of easy-to-synthesize and low-toxicity Zn^{2+}-selective sensors is still a challenging task. In addition, the Cd^{2+} ion usually interferes with the Zn^{2+}-sensing processes and causes spectral changes after interaction with chemosensors similar to that when Zn^{2+} interacts with the chemosensors.[10] Therefore, there is a great need for the design and synthesis of such chemosensors, which have a small molecule and high sensitivity, and can exhibit real-time detection in biological systems and discriminate between Zn^{2+} and Cd^{2+} at physiological pH.

Herein we synthesized a new 8-aminoquinoline derivative **L1** bearing the *ortho*-aminophenol group as a receptor, which shows high sensitivity and selectivity for Zn^{2+} over other possible competitive cations, on the basis of an internal charge transfer (ICT) and chelation-enhanced fluorescence (CHEF) mechanism. The introduction of a carboxamido group is of advantage to the deprotonation of the 8-amino group.[11] Moreover, the *ortho*-aminophenol group provides another two binding sites for coordination, which enhances the high selectivity of the sensor towards Zn^{2+} over other metal ions.

Results and Discussion

Compound **L1** was easily synthesized in 82% yield by a two-step procedure.[12] The single crystal of **L1** was obtained by slow evaporation in dichloromethane (Figure 1) and **L1** was designed to chelate metal ions through two N atoms of the 8-aminoquinoline unit and the N, O atoms of the *ortho*-aminophenol group.

The coordination of **L1** with Zn^{2+} was investigated by spectrophotometric titration in acetonitrile solution. As shown in Figure 2, the absorbance of **L1** at 240 and 296 nm decreases linearly with increasing concentration of Zn^{2+}. Meanwhile, two new absorption peaks appear at 258 and 362 nm, and their intensity gradually increases upon addition of Zn^{2+}. This is accompanied by three isosbestic points at 248, 278 and 338 nm. These phenomena are expected to correspond to the coordination of **L1** with Zn^{2+}, which extends the conjugated system and results in the ap-

[a] Key Laboratory of Nonferrous Metal Chemistry and Resources Utilization of Gansu Province,
Lanzhou 730000, P. R. China
Fax: 86-931-8912582
E-mail: zengzhzh@yahoo.com.cn
zengzhzh@lzu.edu.cn
[b] Pharmacology Laboratory of Gansu Province, Key Laboratory of Preclinical Study for New Traditional Chinese Medicine, Lanzhou University,
Lanzhou 730000, P. R. China
[c] Department of Chemistry, Lanzhou University,
Lanzhou 730000, P. R. China
Supporting information for this article is available on the WWW under http://dx.doi.org/10.1002/ejic.201100245.

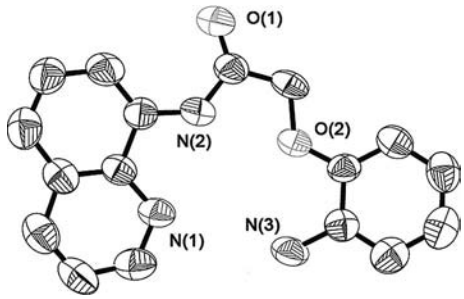

Figure 1. Crystal structure of **L1**. All hydrogen atoms are omitted for clarity (50% probability level for the thermal ellipsoids).

pearance of the new absorption in the long wavelength region.[13] According to the linear Benesi–Hildebrand expression,[14] the measured absorbance [1/(A–A_0)] at 362 nm varies as a function of 1/[Zn^{2+}] with a linear relationship (R^2 = 0.9947), which indicates a 1:1 stoichiometry between Zn^{2+} and **L1** (Figure 2, inset).

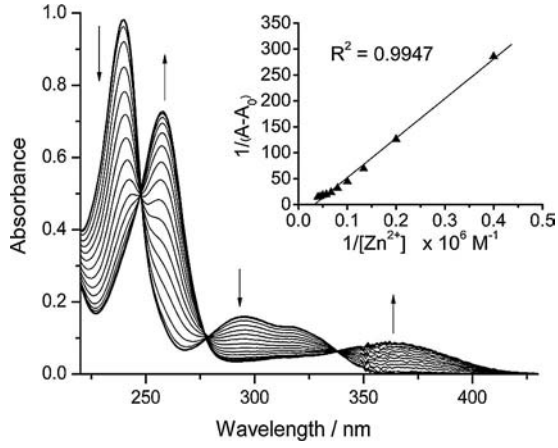

Figure 2. Absorption spectra of **L1** (20 μM) in the presence of Zn^{2+} (0–2 equiv.) in CH_3CN. Inset shows the measured absorbance [1/(A–A_0)] at 362 nm varied as a function of 1/[Zn^{2+}].

Figure 3 shows gradual changes in the fluorescence spectra of **L1** upon addition of Zn^{2+}. As expected, **L1** shows very weak fluorescence (F_0 = 36.5, Φ_0 = 0.006) in acetonitrile solution. Addition of Zn^{2+} (0–20 μM) to the solution of **L1** (10 μM) produces a new emission band centred at 502 nm with a 15.7-fold increase in the fluorescence and a 12.3-fold increase in quantum yield (F = 573, Φ = 0.074). A greenish fluorescence emission of the solution was observed by the naked eye (Figure 3, inset). These results can be explained as follows. After 8-aminoquinoline binds with Zn^{2+}, its intramolecular hydrogen bond breaks and the intramolecular electron-transfer process is forbidden, which enhances the fluorescence emission.[15] Simultaneously, electron transfer from the nitrogen atom of the heterocycle to the metal ion further enhances the ICT process.[16] Another reason for fluorescence enhancement could be that a more rigid structure is formed when Zn^{2+} binds with **L1**. The association constant for Zn^{2+} is estimated to be 3.2×10^4 M^{-1} on the basis of linear fitting of the titration curve by assuming a 1:1 stoichiometry (Figure S1, Supporting Information). This binding mode is also supported by a Job's plot (Figure S2).

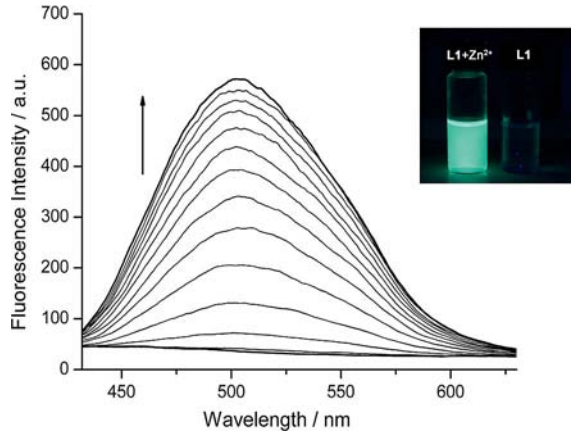

Figure 3. Fluorescence spectra of **L1** (10 μM) excited at 367 nm in acetonitrile solution in the presence of different concentrations of Zn^{2+} (0–2 equiv.). Inset: visible emission observed from **L1** (25 μM) in the absence and presence of Zn^{2+} (50 μM) in CH_3CN.

In order to understand the crucial role of the aminophenol group, which provides additional binding sites for Zn^{2+} ions, the *meta*-aminophenol isomer **L2** of **L1** was synthesized as a control. We tested the fluorescence changes in **L1** and **L2** upon addition of zinc ions (Figures S3 and 4). The fluorescence change between **L1**/Zn^{2+} and **L1** is 4.1 times greater than that between **L2**/Zn^{2+} and **L2** (2 equiv. of Zn^{2+}) in CH_3CN. Moreover, the ^1H NMR spectra of **L1**, **L2**, **L1**/Zn^{2+} and **L2**/Zn^{2+} were recorded. The protons signals for the CONH group and the aromatic rings of the **L1**/Zn^{2+} system all shift to a higher field relative to those of the ligand **L1** (Figure S4). However, for the **L2**/Zn^{2+} system, no apparent changes in the proton signals are seen after the addition of Zn^{2+} (Figure S5). This indicates that the nitrogen and oxygen atoms of the aminophenol unit play an important role in the three-dimensional complexation of Zn^{2+}. We propose a coordination geometry for Zn^{2+} that encompass three N atoms and one O atom.[17] Therefore, we can deduce a possible coordination mode: three N atoms

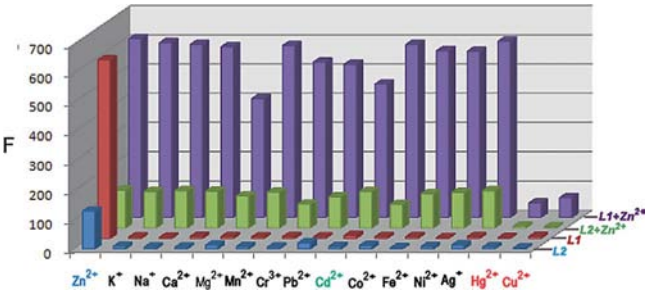

Figure 4. Fluorescence intensities of **L1** (10 μM) and **L2** (10 μM) in the presence of various metal ions and ion mixtures in acetonitrile solution. [K^+] = [Na^+] = [Ca^{2+}] = [Mg^{2+}] = 5 mM, [Zn^{2+}] = [Mn^{2+}] = [Cr^{3+}] = [Pb^{2+}] = [Cd^{2+}] = [Co^{2+}] = [Fe^{2+}] = [Ni^{2+}] = [Ag^+] = [Hg^{2+}] = [Cu^{2+}] = 20 μM. ($\lambda_{ex,\mathbf{L1}}$ = 367 nm, $\lambda_{em,\mathbf{L1}}$ = 502 nm; $\lambda_{ex,\mathbf{L2}}$ = 365 nm, $\lambda_{em,\mathbf{L2}}$ = 494 nm).

and an O atom participate in the coordination environment of Zn^{2+}.

An important property of chemosensors is their high selectivity towards the analyte over the other competitive metal ions. We therefore determined the fluorescence intensity of **L1** at 502 nm in the presence of various metal ions. As shown in Figure 4, only Zn^{2+} gives rise to a prominent fluorescence enhancement of the acetonitrile solution of **L1**, while the other metal ions such as K^+, Na^+, Ca^{2+}, Mg^{2+}, which exist at high concentrations in human cells, do not effect any significant colour or spectral changes. In particular, the addition of Cd^{2+}, known as a typical competitive ion for a Zn^{2+} sensor, does not effect such changes either. However, the fluorescence of the **L1**/Zn^{2+} system was quenched by Cu^{2+} and Hg^{2+}, which may be due to nonradiative energy transition in the process of electron or energy transfer between the d orbital of the ions and the fluorophore.[7,18] These results unambiguously demonstrate the high specificity and selectivity of **L1** for detecting Zn^{2+}. Interestingly, **L2** also exhibits good specificity and selectivity for Zn^{2+} in single and multicomponent systems. The common metals such as K^+, Na^+, Ca^{2+}, Mg^{2+}, Mn^{2+}, Cd^{2+}, Co^{2+}, Fe^{2+}, Ni^{2+}, Cr^{3+} and Ag^+ have a negligible influence on Zn^{2+} sensing. Only, addition of Pb^{2+} elicits tiny fluorescence enhancement, with respect to that for Zn^{2+}, and Cu^{2+} and Hg^{2+} efficiently quench the fluorescence of **L2**/Zn^{2+} system.

The sensing ability of **L1** toward Zn^{2+} at different pH values was investigated (Figure 5). **L1** shows no appreciable fluorescence response to Zn^{2+} in an acidic environment because protonation of the amino group of **L1** weakens the coordination ability of Zn^{2+}.[19] However, **L1** exhibits satisfactory sensing abilities when the pH is increased from 5.5 to 9.0. At pH ca. 7.0, the $F_{\mathbf{L1}+Zn}/F_{L1}$ value reaches a maximum value of 152.5. These data indicate that **L1** could act as a fluorescent probe for Zn^{2+} under physiological pH conditions.

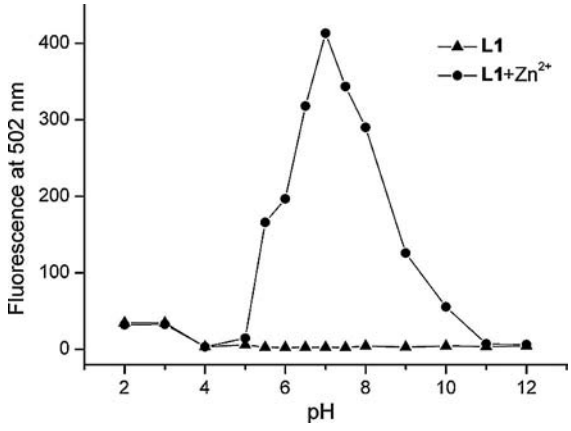

Figure 5. Fluorescence intensities of **L1** (10 μM) in the absence and presence of Zn^{2+} (20 μM) at various pH values in CH_3CN/H_2O (95:5, v/v) (λ_{ex} = 367 nm, λ_{em} = 502 nm).

We also investigated the time evolution of the response of **L1** to 2 equiv. of Zn^{2+} in CH_3CN (Figure S6). We found that the interaction of **L1** with Zn^{2+} was complete in less than 2 min. Therefore, this system could be used for real-time tracking of Zn^{2+} in cells and organisms.

To understand the selectivity and the configuration of **L1**-Zn^{2+}, we carried out density functional theory (DFT) calculations with B3LYP by using the Gaussian 09 package. The 6-31G basis set was used for the H, C, N, O atoms; the exception was for the Zn atom, where the LANL2DZ effective core potential (ECP) was employed. The optimized configuration is shown in Figure 6, which shows that Zn^{2+} ion binds to **L1** very well through four coordination sites, and the whole molecular system forms a nearly planar structure. The Zn–O bond length is 2.10 Å and Zn–N bond lengths are 2.08 Å (Zn–$N_{quinoline}$), 1.98 Å (Zn–$N_{carboxamido}$) and 2.15 Å (Zn–NH_2), respectively. These data indicate that **L1** could provide suitable space to better accommodate corresponding ions.

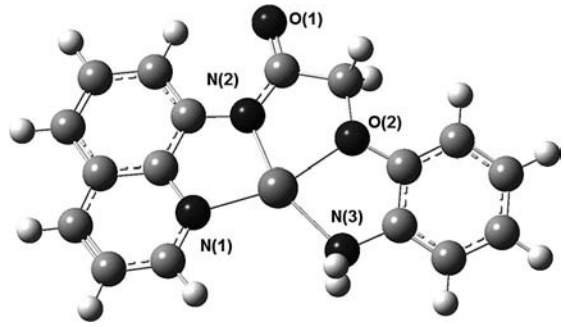

Figure 6. Calculated energy-minimized structure of **L1** with Zn^{2+}.

We then studied the Zn-sensing behaviour of **L1** in living cells. SCaBER cells (human bladder cancer cells) were incubated with 20 μM **L1** for 3 h at 37 °C and show very weak intracellular fluorescence as determined by laser scanning confocal microscopy (Figure 7a). The addition of Zn^{2+} (40 μM) to the treated cells in a culture medium over 0.5 h at 37 °C leads to a significant increase in the fluorescence (Figure 7b). The result indicates that **L1** may be used as a possible sensor to detect intracellular Zn^{2+} in living cells.

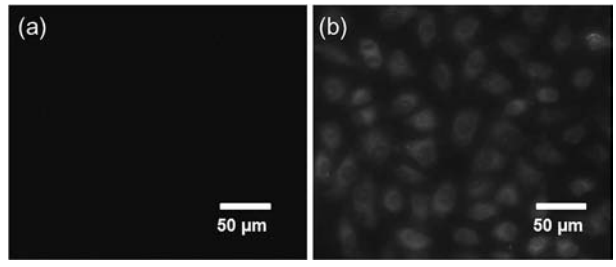

Figure 7. Fluorescence microscope images of SCaBER cells loaded with **L1** incubated for 3 h, (a) without and (b) with the addition of Zn^{2+} (2 equiv.).

Conclusions

A new 8-aminoquinoline-based derivative was synthesized for the detection of Zn^{2+} in living cells. It displays high selectivity, sensitivity and a fast time response to Zn^{2+}.

L1 can discriminate between Zn^{2+} and Cd^{2+} in acetonitrile solution in the physiological pH window and binds to Zn^{2+} through a 1:1 binding mode, which has been confirmed by ESI-MS and DFT calculations. The fluorescent microscopy measurements demonstrate that **L1** is cell permeable. We hope that such Zn^{2+}-selective sensors would have great potential in biomedical and environmental applications.

Experimental Section

Preparation of 2-Chloro-*N*-(quinol-8-yl)acetamide: To a cooled, stirred solution of 8-aminoquinoline (288 mg, 2.0 mmol) and pyridine (0.23 mL, 2.8 mmol) was added dropwise a chloroform solution (10 mL) of 2-chloroacetyl chloride (461 mg, 2.0 mmol) over 1 h. After 2 h at room temperature, a brown–yellow solid was obtained by removing the solvent under reduced pressure. The crude product was purified by silica gel column chromatography by using dichloromethane as eluent to afford 2-chloro-*N*-(quinol-8-yl)acetamide. Yield: 362 mg (80%). ^{1}HNMR ($CDCl_3$, 400 MHz, TMS): δ = 10.92 (s, 1 H), 8.86–8.87 (dd, J = 4, J = 1.6 Hz, 1 H), 8.75–8.86 (m, 1 H), 8.17–8.20 (dd, J = 8, J = 1.6 Hz, 1 H), 7.47–7.59 (m, 3 H), 4.32 (s, 2 H) ppm. ^{13}C NMR ($CDCl_3$, 100 MHz): δ = 164.4, 148.7, 138.7, 136.3, 133.6, 127.9, 127.2, 122.5, 121.8, 116.6, 43.3 ppm.

Preparation of L1: 2-Chloro-*N*-(quinol-8-yl)acetamide, (133 mg, 0.6 mmol), *ortho*-aminophenol (55 mg, 0.5 mmol) and potassium iodide (8 mg) were added to an acetonitrile solution (30 mL). After the solution was stirred and heated at reflux for 10 h under nitrogen, the mixture was cooled to room temperature, and the solvent was removed under reduced pressure to obtain a pale yellow solid, which was purified by silica gel column chromatography by using ethyl acetate/petroleum (1:2, v/v) as eluent to afford **L1**. Yield: 123 mg (83.8%). ^{1}H NMR ($CDCl_3$, 400 MHz, TMS): δ = 11.12 (s, 1 H), 8.77–8.80 (m, 2 H), 8.17–8.20 (dd, J = 8, J = 1.6 Hz, 1 H), 7.55–7.58 (m, 1 H), 7.45–7.48 (dd, J = 8, J = 4 Hz, 1 H), 6.74–6.92 (m, 4 H), 4.75 (s, 1 H), 4.23 (br. s, 1 H) ppm. ^{13}C NMR ($CDCl_3$, 100 MHz): δ = 166.4, 148.5, 145.0, 138.7, 136.42, 136.45, 128.0, 127.3, 122.7, 122.2, 121.7, 118.6, 115.9, 112.4, 68.21 ppm. MS (ESI): m/z = 294.0 [M + H$^+$].

Preparation of L2: Analogous procedures starting with 2-chloro-*N*-(quinol-8-yl)acetamide and *meta*-aminophenol gave **L2**. ^{1}H NMR ($CDCl_3$, 400 MHz, TMS): δ = 10.94 (s, 1 H), 8.86–8.87 (dd, J = 4, J = 1.6 Hz, 1 H), 8.81–8.83 (dd, J = 8, J = 1.6 Hz, 1 H), 8.15–8.18 (d, J = 1.6 Hz, 1 H), 7.54–7.56 (m, 2 H), 7.45–7.48 (dd, J = 8, J = 4 Hz, 1 H), 7.10–7.14 (m, 1 H), 6.37–6.53 (m, 3 H), 4.71 (s, 2 H), 3.72–3.75 (br., 2 H) ppm. ^{13}C NMR ($CDCl_3$, 100 MHz): δ = 167.0, 158.6, 148.6, 148.0, 138.8, 136.2, 133.8, 130.4, 127.8, 127.2, 122.2, 121.7, 116.8, 109.2, 105.0, 102.1, 68.1 ppm. MS (ESI): m/z = 294.2 [M + H$^+$].

X-ray Structure Determinations: Single-crystal X-ray diffraction measurements were carried out on a Bruker SMART 1000 CCD diffractometer operating at 50 KV and 30 mA by using Mo-K_α radiation (λ = 0.71073 Å). The selected crystal was mounted inside a Lindemann glass capillary for data collection with the SMART and SAINT software. An empirical absorption correction was applied by using the SADABS program. All structures were solved by direct methods and refined by full-matrix least-squares on F^2 by using the SHELXTL-97 program package.[20] All non-hydrogen atoms were subjected to anisotropic refinement, and all hydrogen atoms were added in idealized positions and refined isotropically. Crystal data for **L1**: M_r = 293.32, monoclinic, space group $P2(1)/c$, a = 15.022(6) Å, b = 5.256(2) Å, c = 20.586(7) Å, α = 90°, β = 117.58(2)°, γ = 90°, V = 1440.7(10) Å^3, Z = 4, $\rho_{calcd.}$ = 1.352 g cm^{-3}, R_1 = 0.0695 [$I > 2\sigma(I)$]. CCDC-795696 contains the supplementary crystallographic data for this paper. These data can be obtained free of charge from The Cambridge Crystallographic Data Centre via www.ccdc.cam.ac.uk/data_request/cif.

Cell Incubation and Imaging: The SCaBER cells (human bladder cancer cells) were provided by the Cells Bank of Chinese Academy of Science (Shanghai, China). Cells were grown in H-DMEM (Dulbecco's Modified Eagle's Medium, High Glucose) supplemented with 10% FBS (Fetal Bovine Serum) in an atmosphere of 5% CO_2, 95% air at 37 °C. Cells (5×10^8/L) were plated on 18-mm glass coverslips and allowed to adhere for 24 h. Experiments to asses Zn^{2+} uptake were performed in the same media supplemented with 40 μM $Zn(NO_3)_2$ for 0.5 h. Before the experiments, the cells were washed with PBS buffer and then incubated with 20 μM **L1** for 3 h at 37 °C. Cell imaging was then carried out after washing the cells with PBS. The cell images were then captured with a fluorescence-inverted microscope (DMI4000 B, Leica Microsystem) with excitation between 340–380 nm. The total magnification is 400×.

DFT Calculations: The geometry optimizations were carried out in vacuo by using the hybrid density functional Becke-3-Lee–Yang–Parr (B3LYP) potential in conjuration with a 6-31G basis set for the H, C, N, O atoms and a LANL2DZ effective core potential (ECP) basis set for the Zn atom. All the calculations were implemented with the GAUSSIAN 09 software package. Frequency calculations were also implemented for the optimized structure to ensure that the optimized structure was the one which has the lowest energy.

Supporting Information (see footnote on the first page of this article): Materials and general methods, schematic molecular structures, experimental details and additional NMR and ESI-MS data are presented.

Acknowledgments

This study was supported by the Foundation of State Key Laboratory of Applied Organic Chemistry and the NSFC (20171019). Thanks to Shihui Shi for NMR measurements.

[1] a) B. Valeur, I. Leray, *Coord. Chem. Rev.* **2000**, *205*, 3–40; b) K. Rurack, U. R. Genger, *Chem. Soc. Rev.* **2002**, *31*, 116–127; c) V. Amendola, L. Fabbrizzi, F. Foti, M. Licchelli, C. Mangano, P. Pallavicini, A. Poggi, D. Sacchi, A. Taglietti, *Coord. Chem. Rev.* **2006**, *250*, 273–299.

[2] a) A. P. de Silva, D. B. Fox, A. J. M. Huxley, T. S. Moody, *Coord. Chem. Rev.* **2000**, *205*, 41–57; b) Q. W. He, E. W. Miller, A. P. Wong, C. J. Chang, *J. Am. Chem. Soc.* **2006**, *128*, 9316–9317.

[3] a) T. V. O'Halloran, *Science* **1993**, *261*, 715–725; b) J. Y. Koh, S. W. Suh, B. J. Gwag, Y. Y. He, C. Y. Hsu, D. W. Choi, *Science* **1996**, *272*, 1013–1016; c) F. Walker, R. E. Black, *Annu. Rev. Nutr.* **2004**, *24*, 255–275; d) C. J. Frederickson, A. I. Bush, *Biometals* **2001**, *14*, 353–366.

[4] a) K. Kiyose, H. Kojima, Y. Urano, T. Nagano, *J. Am. Chem. Soc.* **2006**, *128*, 6548–6549; b) K. Komatsu, Y. Urano, H. Kojima, T. Nagano, *J. Am. Chem. Soc.* **2007**, *129*, 13447–13454.

[5] a) C. R. Goldsmith, S. J. Lippard, *Inorg. Chem.* **2006**, *45*, 555–561; b) B. A. Wong, S. Friedle, S. J. Lippard, *J. Am. Chem. Soc.* **2009**, *131*, 7142–7152.

[6] a) A. E. Dennis, R. C. Smith, *Chem. Commun.* **2007**, 4641–4643; b) J. F. Zhu, H. Yuan, W. H. Chan, A. W. M. Lee, *Org.*

Biomol. Chem. **2010**, *8*, 3957–3964; c) Z. C. Xu, J. Y. Yoon, D. R. Spring, *Chem. Soc. Rev.* **2010**, *39*, 1996–2006.
[7] K. Rurack, *Spectrochim. Acta Part A* **2001**, *57*, 2161–2195.
[8] P. Jiang, Z. J. Guo, *Coord. Chem. Rev.* **2004**, *248*, 205–229.
[9] a) I. B. Mahadevan, M. C. Kimber, S. F. Lincoln, E. R. Tiekink, A. D. Ward, W. H. Betts, I. J. Forbes, P. D. Zalewski, *Aust. J. Chem.* **1996**, *49*, 561–568; b) P. D. Zalewski, I. J. Forbes, W. H. Betts, *Biochem. J.* **1993**, *296*, 403–408; c) C. J. Frederickson, E. J. Kasarskis, D. Ringo, R. E. Frederickson, *J. Neurosci. Methods* **1987**, *20*, 91–103; d) C. J. Frederickson, *J. Int. Rev. Neurobiol.* **1989**, *31*, 145–238.
[10] a) L. Xue, C. Liu, H. Jiang, *Org. Lett.* **2009**, *11*, 1655–1658; b) E. M. Nolan, S. J. Lippard, *Inorg. Chem.* **2004**, *43*, 8310–83317; c) E. M. Nolan, S. C. Burdette, J. H. Harvey, S. A. Hilderbrand, S. J. Lippard, *Inorg. Chem.* **2004**, *43*, 2624–2635; d) R. Parkesh, T. C. Lee, T. Gunnlaugsson, *Org. Biomol. Chem.* **2007**, *5*, 310–317; e) F. Qian, C. L. Zhang, Y. M. Zhang, W. J. He, X. Gao, P. Hu, Z. J. Guo, *J. Am. Chem. Soc.* **2009**, *131*, 1460–1468.
[11] a) Z. C. Xu, X. H. Qian, J. N. Cui, *Org. Lett.* **2005**, *7*, 3029–3032; b) T. Yang, C. Tu, J. Y. Zhang, L. P. Lin, X. M. Zhang, Q. Liu, J. Ding, Q. Xu, Z. J. Guo, *Dalton Trans.* **2003**, 3419–3424.
[12] Y. Zhang, X. F. Guo, W. X. Si, L. H. Jia, X. H. Qian, *Org. Lett.* **2008**, *10*, 473–476.
[13] Y. Liu, N. Zhang, Y. Chen, L. H. Wang, *Org. Lett.* **2007**, *9*, 315–318.
[14] a) H. A. Benesi, J. H. Hildebrand, *J. Am. Chem. Soc.* **1949**, *71*, 2703–2707; b) M. Barra, C. Bohne, J. C. Scaiano, *J. Am. Chem. Soc.* **1990**, *112*, 8075–8079.
[15] a) K. Hiratani, T. J. Hirose, K. Kasuga, K. Saito, *J. Org. Chem.* **1992**, *57*, 7083–7087; b) T. Yang, C. Tu, J. Y. Zhang, L. P. Lin, X. M. Zhang, Q. Liu, J. Ding, Q. Xu, Z. J. Guo, *Dalton Trans.* **2003**, 3419–3424.
[16] P. J. Jiang, L. Z. Chen, J. Lin, Q. Liu, J. Ding, X. Gao, Z. J. Guo, *Chem. Commun.* **2002**, 1424–1425.
[17] a) H. S. Jung, P. S. Kwon, J. W. Lee, J. II Kim, C. S. Hong, J. W. Kim, S. H. Yan, J. Y. Lee, J. H. Lee, T. Joo, J. S. Kim, *J. Am. Chem. Soc.* **2009**, *131*, 2008–2012; b) Z. X. Li, M. M. Yu, L. F. Zhang, M. Yu, J. X. Liu, L. H. Wei, H. Y. Zhang, *Chem. Commun.* **2010**, *46*, 7169–7171.
[18] K. M. Hendrickson, T. Rodopoulos, P. A. Pittet, I. Mahadevan, S. F. Lincoln, A. D. Ward, T. Kurucsev, P. A. Duckworth, I. J. Forbes, P. D. Zalewski, W. H. Betts, *J. Chem. Soc., Dalton Trans.* **1997**, 3879–3882.
[19] Y. Chen, K. Y. Han, Y. Liu, *Bioorg. Med. Chem.* **2007**, *15*, 4537–4542.
[20] a) G. M. Sheldrick, *SHELXL-97, Program for the Solution of Crystal Structures*, University of Göttingen: Göttingen, Germany, **1997**; b) G. M. Sheldrick, *SHELXL-97, Program for the Refinement of Crystal Structures*, University of Göttingen: Göttingen, Germany, **1997**.

Received: March 10, 2011
Published Online: June 1, 2011

